Field Testing of an Instrument to Measure Near-Surface Currents from Offshore Platforms

Jerry Mullison
RD Instruments Inc.
9855 Businesspark Avenue
San Diego, CA 92131, U.S.A.
jmullison@rdinstruments.com

Caroline Nicholas
Fugro GEOS Inc
PO Box 740010
6100 Hillcroft, Ste. 500
Houston, TX 77274, U.S.A.
c.nicholas@geos.com

Cathryn Primrose
Fugro GEOS Inc
PO Box 740010
6100 Hillcroft, Ste. 500
Houston, TX 77274, U.S.A.
c.primrose@geos.com

***Abstract-* We have carried out extensive field testing of an Acoustic Doppler Current Profiler (ADCP) designed to measure surface currents at ranges of 200-300 m by profiling horizontally from its mounting. The range of vertically profiling ADCPs is well documented, but horizontal profiling from offshore platforms presents unique, less well-understood factors influencing profiling range. These include the potential for interference from other sources on the platform, and that the concentration of scatterers (typically zooplankton) is now relatively uniform over the profiling range. A 300 kHz Horizontal ADCP (H-ADCP), specifically designed with large transducers for maximum range, was deployed from an operating drill ship in the Gulf of Mexico with a stated goal of characterizing its profiling range under varying conditions. The maximum range was determined under a number of possible configurations, which included varying the cell size, bandwidth and mounting depth.**

The H-ADCP presents a unique, simple means for obtaining continuous, real-time horizontal profiles of the near surface currents at significant ranges from an offshore platform. These near surface measurements can not be made with a conventional vertical ADCP due to interference from the platform and its thrusters.

We here present a brief review of the measurement technique followed by a description of the tests performed during the trial. We then present the results from systematic testing intended specifically to empirically characterize the performance of this instrument from an offshore platform.

I. INTRODUCTION

Knowledge of the near surface ocean currents in real time is of great value for the safe accomplishment of a number of offshore operations, including loading / offloading operations, tender docking / undocking and deployment / recovery of subsurface equipment. The Loop Current and its associated eddies in the Gulf of Mexico (GOM) are of particular concern to the offshore industry because they bring sustained high currents with the potential to force the platform off-station and also of inducing vortex-shedding vibrations in the equipment. For safety reasons, drilling risers are generally allowed only a very limited deviation from the vertical (around one or two degrees) at their seabed connection [1]. If the rig is forced off-station to the point that this angle will be exceeded, or if vortex induced vibrations occur in the riser causing stress fatigue at the bottom connection, then the platform must detach from the riser and suspend operations until the event has passed [2].

Satellite altimetry combined with predictive models is widely used in the GOM but it cannot precisely pinpoint the arrival, residence behavior or departure of a high current event at a specific location. For this reason among others, Acoustic Doppler Current Profilers (ADCPs) are used on many offshore platforms in the GOM to provide real-time, on-site measurements of the currents.

The ADCPs in common use offshore are usually of low frequency (for maximum range), and are either suspended from the platform to look downward or mounted on the bottom to look upward. However, for reasons discussed below, these ADCPs cannot measure the near-surface currents that directly affect the platform and its support vessels.

Down-looking ADCPs are typically suspended below the keel of the platform. Bin sizes are typically configured to be 16 or 32 m to achieve maximum range. The combined effect of the deployment depth below the keel, the “blank zone” [3], and the large bin size results in a profile of hundreds of meters, however it is one that starts measuring well below the near-surface currents that will directly affect the platform and its servicing vessels. Simply flipping the instrument over to look upward will not provide the near-surface currents because upward-looking ADCP measurements are subjected to sidelobe contamination [3] near the surface.

Also, these platforms can be very large, and often use thrusters for station-keeping. Therefore any currents measured near the platform itself (by whatever means) will be influenced by the presence of the platform and its thrusters.

RD Instruments (RDI) has developed a Long Range Horizontal ADCP (H-ADCP), Fig. 1, to measure the near-surface currents by looking “sideways” to profile the currents out to ranges beyond the influence of the platform. Fig. 2 is an illustration of one such mount.

We deployed this instrument from a dynamically positioned drill ship on station in the Gulf of Mexico in January, 2003, to characterize its performance in a real world environment.

Fig. 1. Long Range 300 kHz Horizontal ADCP

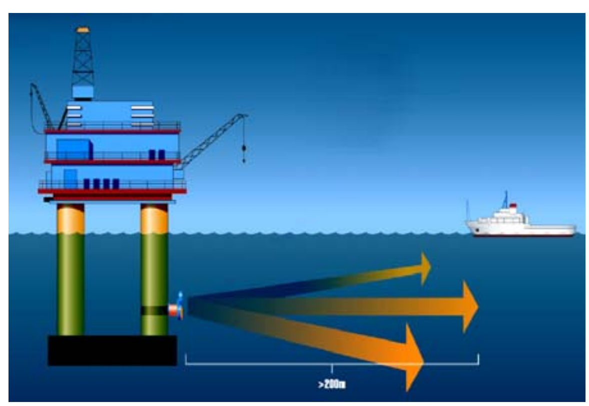

Fig. 2. Conceptual drawing of an H-ADCP as deployed from an offshore platform

II. DEPLOYMENT AND TEST PLAN

Fugro GEOS arranged for the deployment of the H-ADCP on the Global Santa Fe drill ship CR Luigs in late January of 2003 while the vessel was under contract to BHP Billiton and operating in the Gulf of Mexico. The CR Luigs was already equipped with a down-looking ADCP suspended from a dual-winch system developed by Fugro GEOS. A new spreader bar was designed and manufactured to mount the H-ADCP onto the existing deployment frame approximately 10 m above the down-looking ADCP. The deployment setup is pictured in Fig. 3.

There are three user-set parameters that can affect the maximum range measured by the H-ADCP in a given environment:

- The bin size. Choosing larger bin sizes increases the total transmit energy into the water, generally increasing range.
- The bandwidth of the transmitted pulse. The H-ADCP allows the user to choose between 25% and 6% bandwidth for the transmitted pulse. The narrower bandwidth will result in longer range, but requires more averaging than the full 25% bandwidth measurements to get to the same measurement accuracy.
- The deployment depth. Measuring near a boundary raises concerns about interference from the boundary. In addition, ambient noise radiating from the vessel could influence the measurement range.

Our test plan was to systematically vary these parameters and gather data to determine the maximum measurement range with each setup. We chose 4 depths (5, 10, 20 and 27 m), 3 bin sizes (4, 8 and 16 m) and 2 bandwidths (6 and 25%). Due to time constraints we were not able to try all combinations, though we did try to take representative, comparable measurements to determine the effects on range. The tests that we ran are summarized below in Table 1.

TABLE 1
TESTS COMPLETED

Depth\Bin Size	4 m	8 m	16 m
5 m	6 & 25%		
10 m	6 & 25%		
20 m	6 & 25%	6 & 25%	6%
27 m		6%	

Fig. 3. The H-ADCP is suspended above down-looking ADCP and lowered via the dual-winch system.

A minimum of 300 measurements were taken for each of the tests. The number of bins was chosen to set a maximum profiling range of approximately 500 m from the instrument – or well beyond the maximum measurement range we could realistically expect to obtain. Each measurement consisted of one transmit and receive cycle (also known as "single-ping" measurements). Each ping cycle was two seconds because of the range involved and the large number of cells (particularly for the 4 m bin size where 124 bins were measured). Some tests were run with fewer bins (and shorter range) to gather some 1 Hz data; these are presented separately from the range tests. For most tests the data was collected along each of the three beams of the H-ADCP and later converted to an earth-based reference frame.

To determine the maximum range we consider two standard quality control parameters reported along each beam of each measurement: the correlation and the measured Returned Signal Strength Intensity (RSSI). The correlation can be taken as a measure of our confidence in the velocity measurements, while the RSSI shows the range at which the instrument has hit its noise floor [1].

III. RESULTS AND DISCUSSION

A. Bin Size

The effect of the choice of bin size on range was determined by comparing the 6% bandwidth deployments at 20 m depth with 4, 8 and 16 m bins. Each test measured at least 300 profiles of velocity, correlation and returned signal strength intensity (RSSI) among other variables. We averaged the profiles of correlation and RSSI along each beam to form a single representative profile of each variable along that beam. For the measured velocity to be considered reliable RDI recommends its associated correlation value to be at least 64 counts and that its associated RSSI be above its noise floor. At least 2 of the 3 beams of the H-ADCP must satisfy these criteria in order to calculate a two dimensional velocity profile. A simple lookup was performed to determine the last "good" bin – defined as the last bin where at least 2 beams satisfy RDI minimum performance criteria. (An example plot is shown in Fig. 4.) The range to the last good bin for each bin size measured is given in Table 2. Note that no real improvement in range is observed with a 16 m bin size over an 8 m bin size, and we therefore recommend an 8 m bin size for optimal range in this environment.

TABLE 2
RANGE COMPARISON FOR CHANGING BIN SIZE

Bin Size (meters)	Range (meters)
4	181.91
8	193.86
16	193.75

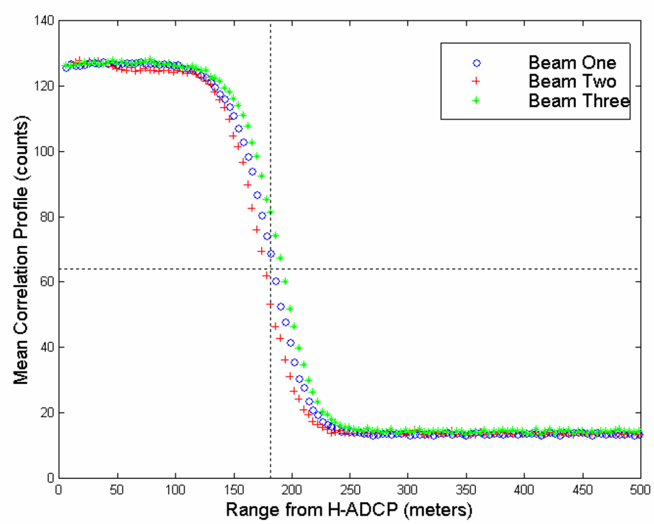

Fig. 4. The lookup process. The 64 count correlation cutoff is shown, along with the last bin where 2 beams report correlations of above 64 counts (181.91 m here).

The correlation value of 64 counts was universally the limiting factor, being reached in every case well before the RSSI measurement reached the transducer's noise floor. This was unexpected, and we believe that it is the result of the ambient noise present in this environment. Dynamically positioned drill ships have high background noise levels. The CR Luigs has 6 thrusters which are always on, and vary significantly in both direction and magnitude of thrust. In addition, the drilling operation itself is quite noisy, and we observed the hull directly inputting energy to the water. Note the capillary wave structure in Fig. 5.

B. Bandwidth

RDI ADCPs generally operate in what RDI calls broadband mode. This Doppler profiling method uses a coded pulse with a fairly broad bandwidth of 25%. In general, broader bandwidth measurements result in higher measurement precision. However, in some situations this precision can be traded for longer range measurements by narrowing the bandwidth of the transmitted pulse. H-ADCPs allow the user to select between broadband coded pulses of 6% or 25%. The 6% bandwidth should be chosen if range is of primary importance, while the 25% bandwidth should be chosen if high resolution in space or time is of primary importance.

Table 3 lists the maximum range comparisons for changing bandwidth. The 6% bandwidth mode offers an increase in range of approximately twenty percent over the 25% bandwidth mode.

TABLE 3
RANGE COMPARISON FOR CHANGING BANDWIDTH

Depth	Bin Size	25% Bandwidth	6% Bandwidth
5	4	149.91	185.91
10	4	141.91	165.91
20	4	153.91	181.91
20	8	161.86	193.86

Fig. 5. Capillary wave structure near the hull of the CR Luigs shows the direct input of energy to the water.

C. Depth

We gathered data at 5, 10, 20 and 27 m deployment depths. The last depth was the limit of our cable range. The H-ADCP measures temperature to incorporate changes in the speed of sound, and we believe that the 27 m deployment depth was below the base of the mixed layer because the temperature measured was roughly one degree Celsius lower than the temperature recorded at the shallower depths. Since our goal was to measure the near-surface currents, we have not included the results from the 27 m deployment here. We present the results from the shallower three depths in Table 4. Only the 4 m bins were tested at all depths of interest.

TABLE 4
RANGE COMPARISONS FOR CHANGING DEPTH

Depth	25% Bandwidth	6% Bandwidth
5 m	149.91	185.91
10 m	141.91	165.91
20 m	153.91	181.91

At first glance, it appears that the 5 m deployment depth is optimal. However, the maximum range measurements do not present the complete picture here. In our deployment we saw immediately that one of the H-ADCP transducers was measuring directly into a thruster wash from the dynamic positioning system. This resulted in anomalously high RSSI and correlation measurements along this beam, probably due to a high concentration of bubbles. The thruster wash was clearly visible at all deployment depths, but the effects were so strong at the 5 m deployment depth that most of the velocity field measured at this depth was unusable.

We believe that we acquired profiles of greater range from the deployment at 20 m because we were dropping below the influence of the vessel and its thrusters. In support of this idea we note that the noise floor was a few counts lower at 20 m than it was at 5 or 10 m. An example RSSI plot is shown in Fig. 6.

D. Velocity Measurements

One primary goal of this deployment was to empirically characterize the range performance of the H-ADCP in a real-world environment, and we have discussed this extensively. However, a second and perhaps more important goal was to develop an effective velocity profiling strategy to measure the near-surface currents in real-time for the platform. We turn to this goal now.

The biggest problem we faced was the nearly omnipresent vortices from the thrusters. The H-ADCP was deployed from the port side of the CR Luigs, with beam three pointing directly out from the ship, beam one at twenty degrees forward and beam two at twenty degrees aft (Fig. 7).

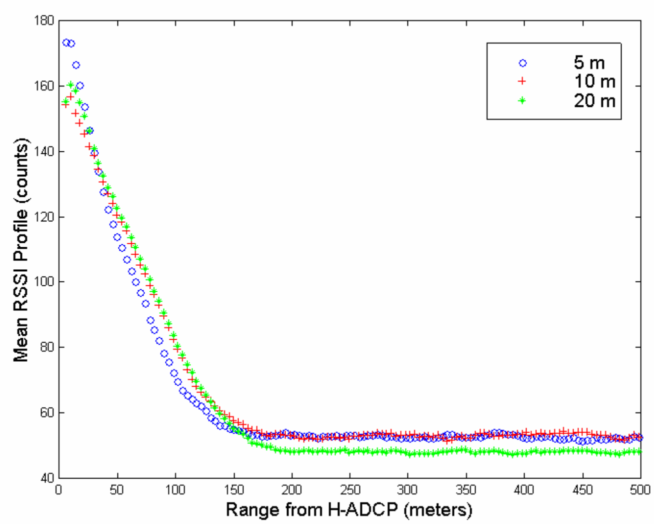

Fig. 6. Returned Signal Strength Intensity variation with depth. The deployments at 5 and 10 m are very similar, but the same transducer at 20 m has its noise floor lowered by about 5 counts.

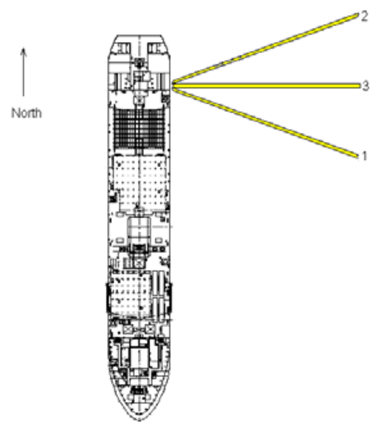

Fig. 7. Plan view of the CR Luigs with the beam patterns from the H-ADCP drawn in. The vessel was usually oriented such that the H-ADCP was pointing eastward.

We show in Fig. 8 the average velocity magnitude and direction from a high resolution profile gathered at the 20 m deployment depth. This plot was prepared by converting the along beam velocities to earth coordinates using the known beam geometry and the output of the H-ADCP compass heading. For quality control an arbitrary minimum of 50 "good" measurements (that is, measurements not flagged "bad" in H-ADCP internal quality control) was set to include the measurement at any given range. The general direction of the current was eastward, which for this deployment means that the main current flow direction was from behind the vessel and broadside-on to it. We also noted that there was something "odd" about the profiles at ranges between 50 and 100 m from the vessel which merited further investigation.

To investigate possible causes of the deviations in this profile we investigated the raw beam data. Contours of these beam coordinate profiles are presented in Fig. 9. The beams are presented from left to right, which is aft to forward in Fig. 7. It is apparent from the raw beam data that beam two is measuring tremendous thruster activity at ranges of 50 to 100 m. Also, we see activity in the far ranges measured by beam three as well. This is consistent with vortices being generated by the thrusters and advecting by the mean surface current first through beam two and then beam three.

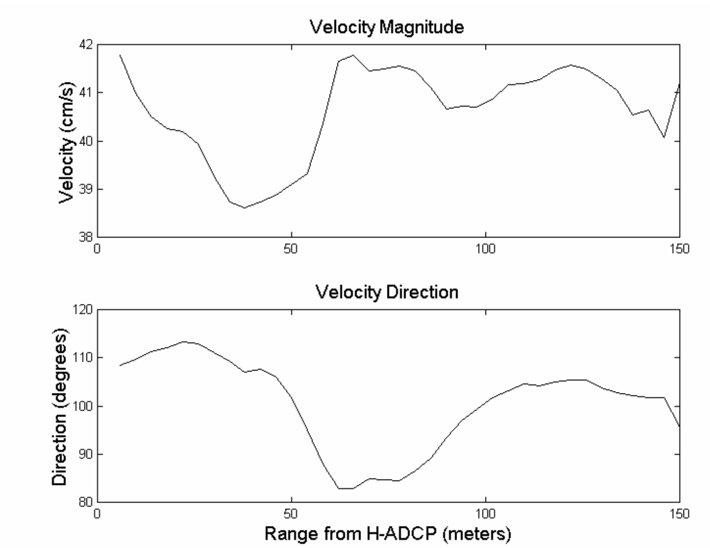

Fig. 8. Average of the velocity magnitude and direction prepared from the data gathered at 20 m depth with 4 m bin size and in 25% bandwidth mode.

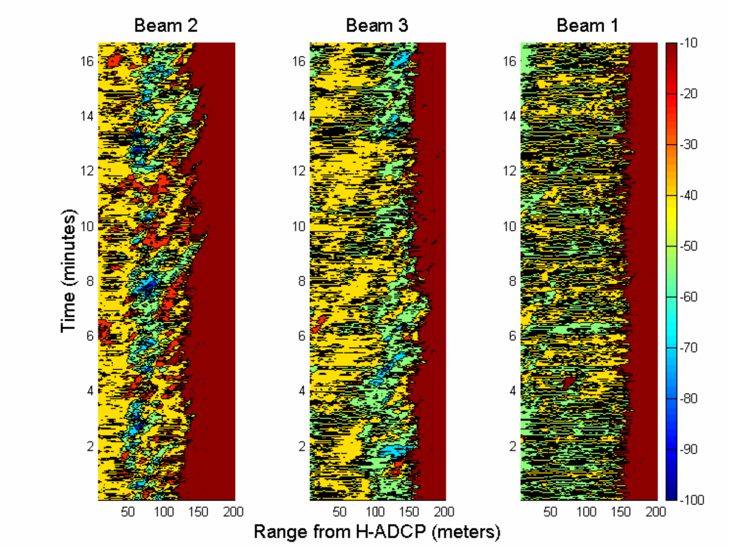

Fig. 9. Raw velocity (in cm/s) as measured along each beam. There is considerable thruster activity at mid-ranges in beam 2 and in the far ranges of beam 3. The maroon color at the far ranges indicates no data.

One of the fundamental assumptions associated with velocity profile measurements from any ADCP is that all beams are measuring homogeneous flow. This is clearly not the case here. RDI provides a measurement of the homogeneity of the flow using its redundant transducer geometry to make a measurement they term the "error velocity". We next consider error velocity in more detail with an eye to using it as a measurement of our confidence that we report the true near-surface currents uninfluenced by the vessel or its thrusters.

E. Error Velocity

A homogeneous two-dimensional velocity field can be measured using any two transducers in the H-ADCP. The third beam is redundant, and allows two measurements of one component of the velocity field that can be compared. The extent to which these two measurements agree indicates the homogeneity of the flow field being measured.

We now show how the coordinate transformation is done to convert the 3 beam-coordinate velocities to an orthogonal XY velocity field with associated error velocity. The Y direction is taken along beam three, and the X direction is perpendicular to beam three. The X velocity is obtained from beams one and two only (beam three measures orthogonally to the X direction), and is obtained from:

$$V_x = V_1/(2SIN(\theta)) + V_2/(2SIN(\theta)) \quad (1)$$

Where V_x = Velocity in the X direction
V_1 = Velocity along beam one
V_2 = Velocity along beam two
θ = Beam angle

V_y is determined from all 3 beams as follows:

$$V_y = V_1(1 - x)/(2COS(\theta)) + V_2(1 - x)/(2COS(\theta)) + xV_3 \quad (2)$$

Where x is chosen to minimize the variance in V_y. The variance is the sum of the squares of the coefficients:

$$\sigma^2_y = (1 - x)^2/(2COS(\theta))^2 + (1 - x)^2/(2COS(\theta))^2 + x^2 \quad (3)$$

Setting $\partial\sigma^2_y / \partial x = 0$ determines the value for x that yields the minimum variance.

The error velocity, V_{err}, is a difference of two possible V_y solutions, which are chosen as:

$$V_{err} = V_y(x=1) - V_y(x = 0) \quad (4)$$

Which we restate as:

$$V_{err} = V_1/(2COS(\theta)) + V_2/(2COS(\theta)) - V_3 \quad (5)$$

RDI scales the error velocity so that its variance is equal to the variance in the velocity measured in the X direction. Choosing a scale factor of K and again using the fact that variance equals the sum of the squares of the coefficients yields:

$$\sigma^2_{err} = \sigma^2_x \quad (6)$$

$$K^2/(2COS(\theta))^2 + K^2/(2COS(\theta))^2 + K^2 = 1/(2SIN(\theta))^2 + 1/(2SIN(\theta))^2 \quad (7)$$

which we solve to obtain our scaling factor, K.

We propose that the error velocity can be treated as a bounding function on the measured velocity profiles. It will vary with inhomogeneity in the flow field, such as the vortices we see, and it is scaled appropriately. We show in Fig. 10 the velocity profile from Fig. 8 along with the error velocity portrayed as a bounding envelope. (Strictly speaking, the error velocity was treated as an error estimate on V_x and V_y and brought forward to these magnitude and direction profiles using standard error propagation.)

The effect of the thrusters is clearly evident in the bounding envelope. The large bulge at 50 to 100 m range is due to the vortices present only in beam two. That the error velocity changes sign in going from the mid range to the far range of the measurement is due to the vortices in beam three at the far ranges.

We investigated this further by recalculating the horizontal velocity field using only 2 beams (beams one and three, and beams one and two), and show the results in Fig. 11. We believe that a combination of the 3 solutions represents the best approximation to the true velocity field. Clearly, all of the solutions are in agreement out to a range of about 50 m. In that range all solutions show a decrease in the magnitude of the velocity field and a slight turning in its direction. If we consider the 2-beam solution (discarding beam two) in the range of 50 to 100 m we see a fairly constant magnitude and direction of the velocity field that carries through to the second 2-beam solution (discarding beam three) in the far ranges.

Of course, this type of subjective choosing between solutions at different ranges will not be of much operational use on a working platform, but we propose that simply considering the error velocity as a bound upon the measured velocity gives a simple indication of the ranges at which the 3-beam solution can be trusted (here out to approximately fifty meters, and again at about one hundred meters).

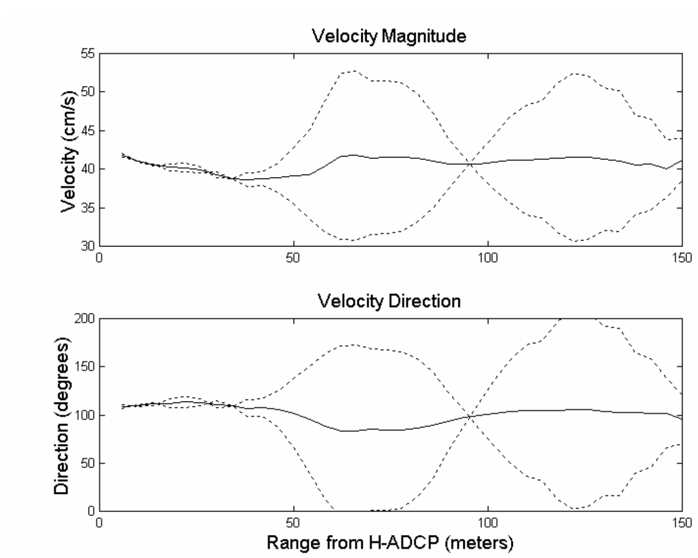

Fig. 10. Velocity magnitude and direction profiles as in Fig. 8, but with the error velocity plotted as a bounding function to give a measure of confidence in our results. The bulges in the bounding envelope are due to the vortices present in beam two and beam three.

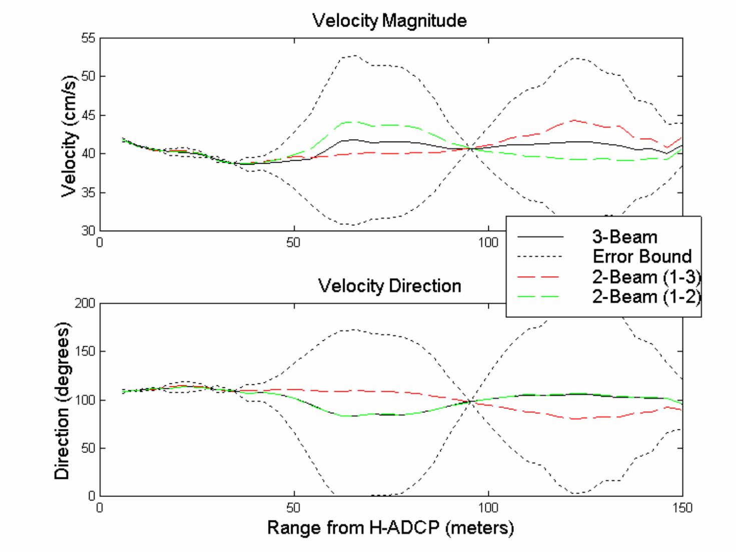

Fig. 11. The velocity and error bound as presented in Fig. 2, with the addition of the velocity field as recalculated using only 2-beam solutions.

The mean current direction is from behind the ship and roughly broadside-on to it. We suspect that the decrease in magnitude and slight change in direction of the velocity profile is due to the presence of the platform and that the "true" near-surface currents are measured at the farther ranges.

IV. FUTURE WORK

When gathering data with 8 m cells and full 25% bandwidth, we noticed what appeared to be ocean swell in the data (Fig. 12). We decreased the range to obtain a 1 Hz data rate and gathered a long time series for wave analysis. RDI has developed a technique in which the measurements of velocities in several bins along each beam are treated as a spatial array of simultaneous measurements of phase at known separations [4]. RDI is currently working on applying this technique to the H-ADCP, and we look forward to applying it to this data set.

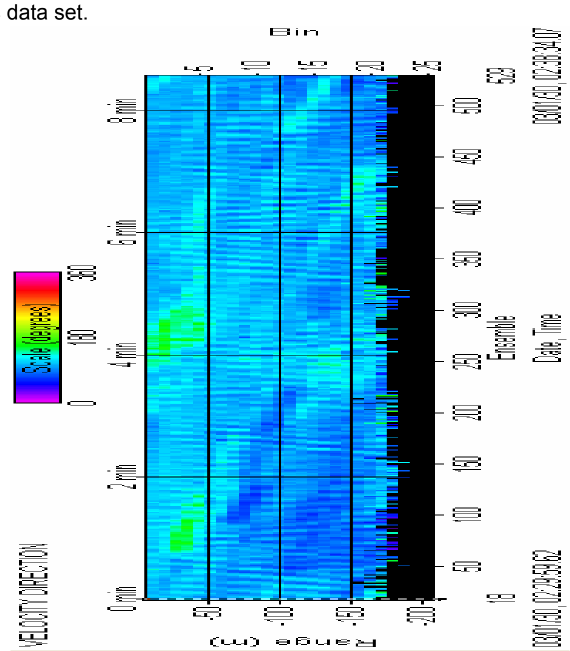

Fig. 12. Contour plot of velocity magnitude. The vertical axis is time in seconds. The two strong features in the near ranges (left) are vortices. The wave field is shown by the nearly horizontal stripes.

V. CONCLUSIONS

We deployed a new Long Range Horizontal ADCP from a dynamically positioned drill ship operating in the deep waters of the Gulf of Mexico. We found that our maximum range was about 200 m, and believe that we were limited by the operational noise of the vessel itself. We determined that an optimal deployment configuration for maximum range in this environment is to deploy it at 20 m depth, with bin size of 8 m and with 6% bandwidth. We believe the 20 m deployment depth is optimal because it is as far from the noise of the platform as we could get while still measuring within the mixed layer.

We found that the vortices from the thrusters were omnipresent, and that they can introduce substantial bias in the mean velocity fields. However, the presence of these vortices was readily identifiable by using the error velocity parameter as a bounding function on the profile. We can use the error velocity to help determine an optimal mounting site to minimize the direct influence of the thrusters on our measurements. Or, if the mounting site cannot be moved, the error velocity can be used to distinguish the velocity ranges influenced by the thrusters from the background velocity.

We found that the mean current direction was generally from behind the platform and broadside-on to it. We also showed that the magnitude of the velocity field tended to decrease over a short range from the ship, and believe that this is due to presence of the platform.

We observed what we believe to be ocean swell in the data. We gathered a high resolution set of data at 1 Hz for later analysis using RDI's directional wave algorithm when it is adapted for H-ADCP for use.

VI. ACKNOWLEDGEMENTS

We would like to thank Global Santa Fe for allowing us to stage this deployment from the CR Luigs. We would also like to thank BHP Billiton to whom the platform was under contract at the time. We would also especially like to thank the officers and crew of the CR Luigs for their help with, and enthusiasm for, these trials.

VII. REFERENCES

[1] American Petroleum Institute. "Design, Selection, Operation & Maintenance of Marine Drilling Riser Systems. API RP 16Q. 1993.

[2] R.E. Steddum: "The Impact of Currents on Offshore Operations, A Drillers Perspective", GOM Currents for Deepwater Operations Workshop Proceedings September 10, 2002

[3] RD Instruments. "Acoustic Doppler Current Profilers – Principles of Operation: A Practical Primer. Second Edition for BroadBand ADCPs". 1996

[4] E.A. Terray, B.H. Brumley and B. Strong: "Measuring waves and currents with an upward-looking ADCP." *Proc. IEEE 6th Working Conference on Current Measurement*, IEEE Press, 66-71. 1999.